

Radial profile of diffusion-controlled He positive columns

T. Kimura, A. Kano, and K. Ohe

Department of Systems Engineering, Nagoya Institute of Technology, Nagoya 466, Japan

(Received 19 April 1995; accepted 22 August 1995)

The radial profile of electron temperature deduced from the measured electron energy distribution function (EEDF) is investigated in an axially homogeneous He positive column and compared with a theoretical one calculated from the electron energy balance equation. The radial shift of the measured EEDF can be explained by the effect of the ambipolar potential. © 1995 American Institute of Physics.

The theory of a diffusion-controlled positive column has been developed using ambipolar diffusion of the charged particles.¹⁻⁴ The radial profile of the electron density is approximated by the zeroth-order Bessel function-like by assuming a uniform Maxwellian electron energy distribution over the column. However, the electron energy distribution function (EEDF) observed even in inert gases such as He and Ne shifts from the Maxwellian, being approximated by a two-temperature function.^{5,6} The discrepancy from the Maxwellian produces quantitative disagreement between theory and the experiment. The non-Maxwellian EEDF has been taken into account in some theories.⁷⁻⁹

The averaged energy estimated from the EEDF observed in a Ne positive column decreases in the radial direction.⁶ Ilic¹⁰ has successfully predicted, except for high pR , where p is the gas pressure and R the tube radius, such a variation of the electron temperature by using the three moment equations for Maxwellian electrons and ions. The discrepancy for high pR remains to be solved. To reduce the discrepancy, the radial variations of the energy gain and loss processes for non-Maxwellian electrons should be included in the electron energy balance equation.

There are two aims in the present paper: (1) to compare the radial profile of the electron energy calculated from the energy balance equation with the experimental profile, and (2) to investigate the influence of the ambipolar diffusion and the electric field on the electron energy by using the measured EEDF.

A discharge tube with 50 mm inner diameter ($2R=50$ mm) and 360 mm length is used, filled with He gas pressure 0.40 Torr. The discharge current I_d is varied from 20 to 150 mA, where the positive column is striation-free. Two single cylindrical probes of 0.15 mm in diameter and 2 mm in length, which are movable in the radial direction, are installed at a position 170 and 220 mm from the anode, respectively. The EEDF is detected using the former probe, and the axial electric field E_z ($=1.9$ V cm⁻¹) is detected as a difference of the floating potentials between the probes.

A ramp voltage ($V_{p-p}=40$ V) of 0.65 Hz to sweep the probe bias voltage V_p is applied to the anode and the cathode. Since the probe is connected with the ground, such a voltage can sweep V_p . The probe current i_p , which is converted into the voltage by an operational amplifier, is fed to an AD converter with 16-bit resolution and 4096 words to digitize the signals by 0.2 ms sampling period. The EEDF

$[=F(\epsilon)]$ can be measured by the well-known Druyvesteyn method¹¹ by detecting the second derivative i_p'' of i_p with respect to V_p . The electron energy probability function (EEDF) $f(\epsilon)$ $[=F(\epsilon)\epsilon^{-1/2}]$ is obtained with a finite impulse response filter method.⁵ From the cutoff frequency of the filter, the measurement error in the EEDF can be estimated within 10% from 15 to 22 eV.

The theoretical EEDF $f_B(\epsilon)$ is calculated for the homogeneous steady-state Boltzmann equation corresponding to that at the tube center. The equation is deduced by taking account of the elastic and the inelastic collisions as¹²

$$2 \frac{m_e}{M} N Q_d \epsilon^2 f_B(\epsilon) + \frac{E_z^2 \epsilon}{3 N Q_T} \frac{d}{d\epsilon} [f_B(\epsilon)] + \sum \int_{\epsilon}^{\epsilon+\epsilon_j} N Q_j \epsilon f_B(\epsilon) d\epsilon + \int_{\epsilon}^{\epsilon+\epsilon_i} N Q_i \epsilon f_B(\epsilon) d\epsilon = 0, \quad (1)$$

where N is the neutral atom density, m_e/M the mass ratio of electron to the atom, Q_d is the momentum transfer cross section, and Q_T is the total cross section. The cross sections Q_j ($j=1-3$), whose threshold energies are ϵ_j ($j=1-3$), correspond to direct excitations of 2^1S+2^3S , 2^3P and 2^1P levels, respectively, and that of Q_i , whose threshold energy is ϵ_i , corresponds to direct ionization. These values are referred to in the literature.^{13,14}

It is known that the EEDF $f(\epsilon)$ measured at the center agrees well with that calculated for the He positive column (see Fig. 3), and can be approximated by the two-temperature function, whose expression is given by Callis and Tuma,¹⁵ as follows:

$$f(\epsilon) = A_0 \exp(-q\epsilon/T_b) \quad (\epsilon < \epsilon_1), \\ = A_0 \exp(-q\epsilon_1/T_b) \exp[-q(\epsilon - \epsilon_1)/T_t] \quad (\epsilon_1 < \epsilon), \quad (2)$$

where T_b and T_t are the bulk and the tail temperature, respectively, and A_0 is a coefficient determined so as to satisfy $\int_0^\infty \epsilon^{1/2} f(\epsilon) d\epsilon = 1$. The temperatures T_b and T_t in the experiment are approximately estimated as $T_b=5.4$ eV and $T_t=1.4$ eV, respectively.

The radial profiles of the plasma potential $\Phi(r)$ and the temperatures $T_b(r)$ and $T_t(r)$ are measured as shown in Figs. 1(a) and 1(b), respectively, where r is the coordinate from the tube center to the wall. The profile of $\Phi(r)$, which is determined with respect to the potential at the center, can

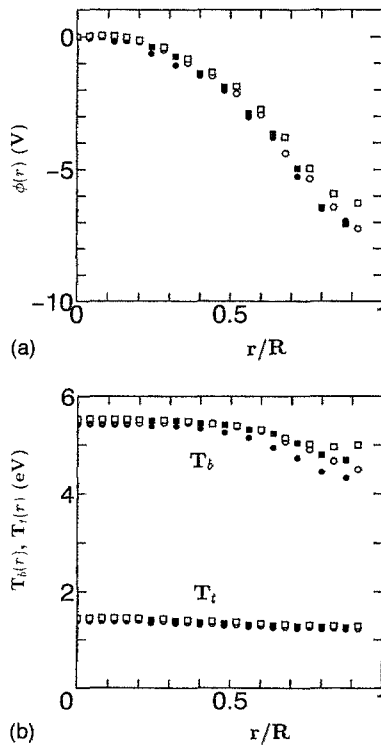


FIG. 1. Radial profiles of $\Phi(r)$ in (a) and that of T_b and T_i in (b), where \circ is $I_d=150$ mA, \bullet is 80 mA, \square is 40 mA, and \blacksquare is 20 mA.

be approximated by the equation $T_b(r) \ln[n_e(r)/n_e(0)]/q$, where $n_e(r)$ is the radial electron density. The temperature $T_b(r)$ decreases in the radial direction, whereas $T_i(r)$ remains approximately constant. Little dependence of these radial profiles on I_d is detected over the measured I_d .

The variation $T_b(r)$ is deduced from the energy balance equation under the following assumptions.

- (1) Electrons and ions move in the radial direction obeying ambipolar diffusion. Then, the radial velocity $v_r(r)$ of the charged particles is given by $\mu_i E_r(r)$, where the radial electric field $E_r(r) = -d\Phi(r)/dr$ is estimated as $[T_b(r)/q] \{ [dn_e(r)/dr]/n_e(r) \}$, since the relation $|[1/T_b(r)] dT_b(r)/dr| \ll |[1/n_e(r)] dn_e(r)/dr|$ holds in our experiment. The ion mobility μ_i is $0.92/p$ ($\text{m}^2 \text{s}^{-1} \text{V}^{-1}$).¹⁶
- (2) The radial profile of $n_e(r)$ is given by the zeroth-order Bessel function.
- (3) The tail temperature $T_i(r)$ is independent of the radial position, in contrast to $T_b(r)$.
- (4) The electron energy losses due to the elastic, the excitation, and the direct ionization collisions are taken into account, while those due to the stepwise ionization and Coulomb collisions are neglected. Since the metastable density is about $1-5 \times 10^{11} \text{cm}^{-3}$ for our experiment, the energy loss due to the collision between electrons and metastables is much smaller than that due to the excitation one.
- (5) The gas temperature is uniform in the radial direction, referring to a previous paper.¹⁷

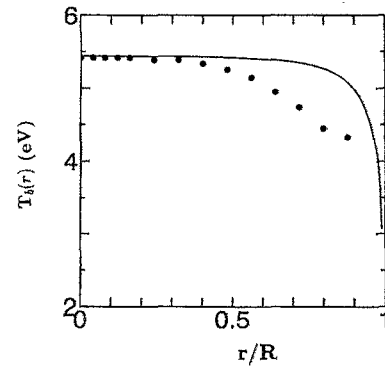


FIG. 2. Comparison of the measured $T_b(r)$ with the calculated one for $I_d=150$ mA, where the solid line is the calculated $T_b(r)$.

Then, the energy balance equation for electrons is deduced as

$$\frac{\partial}{\partial r} \left(v_r(r) \frac{5}{2} T_b(r) \right) = q \frac{3}{2} \mu_i E_r^2(r) + q \mu_e E_z^2 - \epsilon_1 N v_1(r) - \epsilon_i N v^I(r) - \frac{3m_e}{M} \nu_m T_b(r), \quad (3)$$

where μ_e is the electron mobility, which is $86/p$ ($\text{m}^2 \text{s}^{-1} \text{V}^{-1}$).¹⁸ The second term in Eq. (3) is approximated as $-5\mu_i E_r(r)^2/2$. The elastic frequency ν_m is evaluated as

$$\frac{3m_e}{M} T_b(0) \nu_m = \frac{3}{2} q \mu_i E_r^2(0) + q \mu_e E_z^2 - N v_1(0) \epsilon_1 - N v^I(0) \epsilon_i - \frac{5}{2} T_b(0) \left. \frac{dv_r(r)}{dr} \right|_{r=0}. \quad (4)$$

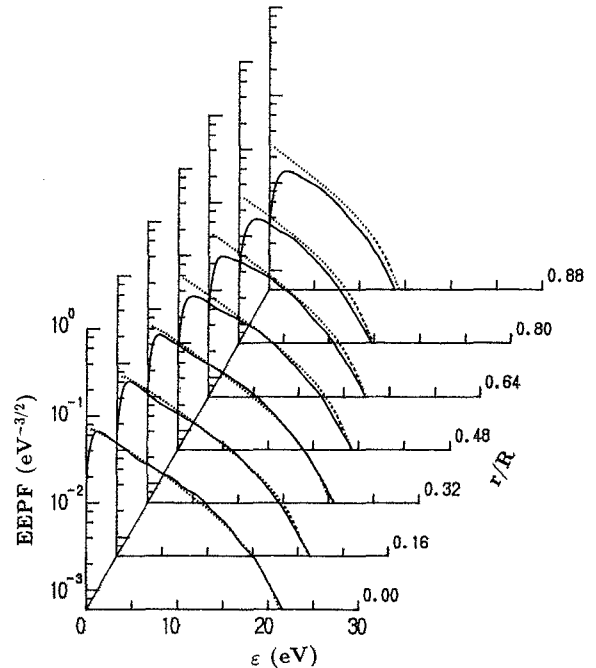


FIG. 3. Radial dependence of $f(\epsilon)$ and $f_B(\epsilon)$ at $p=0.4$ Torr and $I_d=150$ mA, where the solid lines are $f(\epsilon)$ and the dotted ones are $f_B(\epsilon)$.

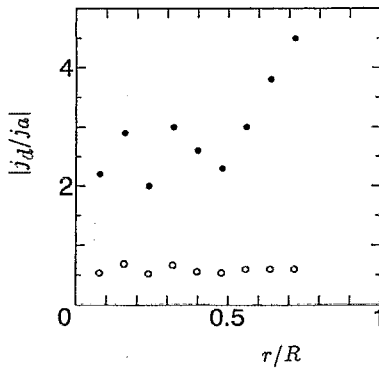


FIG. 4. Radial dependence of ratio $|j_d/j_a|$, where ○ is to 5 eV and ● is to 15 eV.

The excitation rate ν_1 to the 2^1S+2^3S level and the ionization rate ν^I are, respectively, estimated as¹⁵

$$\nu_1(r) = 5.6 \times 10^{-21} \sqrt{\frac{2q}{\pi m_e}} \left(\frac{T_t}{T_b(r)} \right)^2 \sqrt{\frac{T_b(r)}{q}} \times \exp\left(-\frac{q\epsilon_1}{T_b(r)}\right), \quad (5)$$

$$\nu^I(r) = 7.4 \times 10^{-21} \sqrt{\frac{2q}{\pi m_e}} \left(\frac{T_t}{T_b(r)} \right)^2 \sqrt{\frac{T_b(r)}{q}} \times \exp\left(-\frac{q\epsilon_1}{T_b(r)}\right) \exp\left(-\frac{q(\epsilon_i - \epsilon_1)}{T_t}\right). \quad (6)$$

Equation (3) can be numerically solved using the initial values of $T_b(0)$ and $T_t(0)$, which are estimated from the experiment, as shown in Fig. 2. Qualitative agreement between the measured and calculated $T_b(r)$ is obtained, leaving a quantitative discrepancy. The discrepancy may be partially attributed to the neglect of the processes related to the metastables such as the energy loss due to the stepwise ionization and the energy gain due to the superelastic collision. Since the metastable density n_m decreases more gradually than the zeroth-order Bessel distribution¹⁹ and the ratio of n_m to n_e is about 30 for our experiment, the influence of the metastables on $T_b(r)$ is negligible. Thus, the discrepancy indicates that there is an intrinsic problem in estimating the energy loss, which is the deceleration of electrons to the wall by the potential barrier. The further theoretical and experimental investigations of the radial variation of $f(\epsilon)$ will be necessary.

The radial dependence of $f(\epsilon)$ at $I_d=150$ mA and $p=0.40$ Torr is shown in Fig. 3, where the radial dependence of $f_B(\epsilon)$ approximated by $f_B[\epsilon + \Phi(r)]$ is shown as well. In Fig. 3, the EEPFs $f(\epsilon)$ and $f_B(\epsilon)$ are normalized to $\int_0^\infty \epsilon^{1/2} f(\epsilon) d\epsilon|_{r/R=0} = 1$ and $\int_0^\infty \epsilon^{1/2} f_B(\epsilon) d\epsilon|_{r/R=0} = 1$, respectively. The agreement between $f(\epsilon)$ and $f_B(\epsilon)$ at all r/R shows that only a group of electrons overcoming the poten-

tial barrier $\Phi(r)$ can diffuse toward the wall. Of course, the low-energy electrons that have a energy less than $\Phi(r)$ cannot reach the position r , but they are reflected toward the tube axis by $\Phi(r)$, as predicted by the previous papers.²⁰⁻²²

Now, we discuss the possibility to yield quantitative discrepancy by the measured $f(\epsilon)$ and $\Phi(r)$. The component of the radial current density may be divided into the advective drift one j_a toward the tube axis and the diffusion one j_d to the wall. The current densities j_a and j_d can be approximately deduced as $j_a = [q\epsilon^{1/2}/m_e \nu_m(\epsilon, r)] E_r(r) f(\epsilon)$ and $j_d = [2q\epsilon/3m_e \nu_m(\epsilon, r)] \{d[f(\epsilon)\epsilon^{1/2}]/dr\}$ from the radial variation of $f(\epsilon)$ measured, respectively.²² Here, the coefficients $q/m_e \nu_m(\epsilon, r)$ and $2q\epsilon/3m_e \nu_m(\epsilon, r)$ correspond to the electron mobility and the electron diffusion coefficient at ϵ , respectively. Since the sum of j_a and j_d is the radial density at ϵ , the total radial current density is deduced from integrating j_a and j_d . The diffusion cooling is dominant for $j_d > j_a$, while the advective Joule heating is for $j_a > j_d$. Figure 4 shows the radial dependence of the ratio $|j_d/j_a|$ for typical low $\epsilon (=5$ eV) and high $\epsilon (=15$ eV), where $|j_d/j_a|$ are $[2(5)^{1/2}/3E_r(r)f(5)] \{d[f(\epsilon)\epsilon^{1/2}]/dr\}_{\epsilon=5 \text{ eV}}$ and $[2(15)^{1/2}/3E_r(r)f(15)] \{d[f(\epsilon)\epsilon^{1/2}]/dr\}_{\epsilon=15 \text{ eV}}$ by using the measured $f(\epsilon)$ and $E_r(r)$, respectively. The predominance of the joule heating for low ϵ causes the electron movement by the acceleration to the axis due to $E_r(r)$, while that of the diffusion cooling for high ϵ results in the movement by the deceleration to the wall.

In conclusion, the conventional hydrodynamic equation cannot quantitatively describe the radial dependence of the electron energy. The quantitative discrepancy between the experiment and the theory is attributed to the difference between the electron movements for low- and high-energy electrons.

¹W. Schottky, Phys. Z. **25**, 635 (1924).

²J. R. Forrest and R. N. Franklin, Br. J. Appl. Phys. **17**, 1569 (1966).

³S. A. Self and H. N. Ewald, Phys. Fluids **9**, 2486 (1966).

⁴V. Martisovits, J. Phys. B Atom. Mol. Phys. **3**, 850 (1970).

⁵T. Kimura, A. Yoneya, and K. Ohe, Jpn. J. Appl. Phys. **30**, 1877 (1991).

⁶D. Hermann, A. Rutscher, and S. Pfau, Beitr. Plasmaphys. **11**, 75 (1971).

⁷K. Masek and T. Ruzicka, Czech. J. Phys. B **21**, 43 (1971).

⁸C. M. Ferreira, J. Appl. Phys. **54**, 2261 (1983).

⁹J. Loureiro and C. M. Ferreira, J. Phys. D Appl. Phys. **22**, 1680 (1989).

¹⁰D. B. Ilic, J. Appl. Phys. **44**, 3993 (1973).

¹¹M. J. Druyvesteyn, Z. Phys. **64**, 790 (1930).

¹²W. R. L. Thomas, J. Phys. B Atom. Mol. Phys. **2**, 551 (1969).

¹³L. L. Alves and C. M. Ferreira, J. Phys. D Appl. Phys. **24**, 581 (1991).

¹⁴M. Hayashi (private communication, 1992).

¹⁵R. W. Callis and D. T. Tuma, IEEE Trans. Plasma. Sci. **PS-2**, 283 (1974).

¹⁶J. A. Hombeck, Phys. Rev. **84**, 615 (1951).

¹⁷A. Seto, A. Nishitsuji, and A. Sakaguchi, Trans. IEEE Jpn. **103**, 357 (1983) (in Japanese).

¹⁸R. A. Nielsen, Phys. Rev. **50**, 950 (1936).

¹⁹Y. Ichikawa and S. Teii, J. Phys. D Appl. Phys. **13**, 1243 (1980).

²⁰L. D. Tsendin and Y. B. Golubovskii, Sov. Phys. Tech. Phys. **22**, 1066 (1977).

²¹I. B. Bernstein and T. Holstein, Phys. Rev. **94**, 1475 (1954).

²²M. J. Hartig and M. J. Kushner, J. Appl. Phys. **73**, 1080 (1993).